nature communications

Article

https://doi.org/10.1038/s41467-025-59168-5

Remdesivir, mAb114, REGN-EB3, and ZMapp partially rescue nonhuman primates infected with a low passage Kikwit variant of Ebola virus

Received: 15 January 2025

Accepted: 12 April 2025

Published online: 23 April 2025

Check for updates

Abhishek N. Prasad[1,2], Courtney Woolsey[1,2], Viktoriya Borisevich[1,2], Krystle N. Agans[1,2], Daniel J. Deer[1,2], Joan B. Geisbert[1,2], Mack B. Harrison[1,2], Natalie S. Dobias[1,2], Karla A. Fenton[1,2], Robert W. Cross[1,2] & Thomas W. Geisbert[1,2]

In 2018, a clinical trial of four investigational therapies for Ebola virus disease (EVD), known as the PALM trial, was conducted in the Democratic Republic of Congo. All patients received either the antiviral remdesivir (RDV) or a monoclonal antibody product: ZMapp, mAb114 (Ebanga), or REGN-EB3 (Inmazeb). The study concluded that both mAb114 and REGN-EB3 were superior to ZMapp and RDV in reducing mortality from EVD. However, the data suggested that some patients in the RDV and ZMapp groups might have been sicker at the time of treatment initiation. Here, we assessed the efficacy of each of these therapies in a uniformly lethal rhesus monkey model of EVD when treatment was initiated 5 days after Ebola exposure. Treatment with RDV, mAb114, REGN-EB3, and ZMapp each resulted in similar survival (approximately 40%). Survival was associated with circulating viral load at treatment initiation. A trend of more escape mutants in the GP1 and GP2 domains was observed for the mAb114 group. Our data show similar suboptimal efficacy of individual therapeutics in the uniformly lethal NHP model of EVD, supporting further clinical investigation of therapeutic combinations to maximize the overall therapeutic effect and improve patient outcomes, particularly for the treatment of advanced stage EVD.

The family *Filoviridae* consists of several genera of non-segmented negative strand RNA viruses, some of which are capable of causing severe and often fatal disease in humans[1]. Namely, viruses within the genera *Orthoebolavirus* and *Orthomarburgvirus* can cause lethal hemorrhagic disease in humans known as Ebola disease (EBOD) and Marburg disease, respectively, with case fatality rates up to 90%[1,2]. Within the *Orthoebolavirus* genus, virus members of four species are known to have caused disease in humans: *Orthoebolavirus bundibugyoense* (Bundibugyo virus; BDBV), *Orthoebolavirus sudanense* (Sudan virus; SUDV), *Orthoebolavirus taiense* (Taï Forest virus; TAFV), and *Orthoebolavirus zairense* (Ebola virus; EBOV). EBOV has posed the most significant threat to public health, with several major outbreaks over the past decade. Notably, the 2013-16 West African epidemic of EBOV resulted in 28,600 cases with 11,325 deaths[3], while the 2018-2020 EBOV outbreak in the Democratic Republic of Congo (DRC) caused 3,481 cases and 2,299 deaths[4].

[1]Galveston National Laboratory, University of Texas Medical Branch, Galveston, TX, USA. [2]Department of Microbiology and Immunology, University of Texas Medical Branch, Galveston, TX, USA. e-mail: twgeisbe@utmb.edu

Prior to 2013, known outbreaks of human disease caused by filoviruses were sporadic, often separated by years, and geographically limited in spread outside of the initial foci of infection. The increased incidences of EBOV and other filovirus outbreaks have resulted in renewed interest in fast-tracking vaccines and therapeutics for rapid deployment in the event of an outbreak, which remain difficult if not impossible to predict given large gaps in our understanding of the natural ecology of filoviruses[5,6]. Substantial progress has been made in developing preventive vaccines and postexposure treatments against EBOV[7–9]. In addition to monoclonal antibodies (mAb), two of which are currently licensed for human use[10,11], small-molecule antivirals such as remdesivir (GS-5734), a monophosphoramidate prodrug of an adenosine nucleoside analog, have shown therapeutic benefit in nonhuman primate (NHP) models of advanced (i.e., at or following the point of detectable viral replication) filovirus infection[12–18], including for EBOV[17,19–23], and thus have been encouraging as potential countermeasures to filovirus disease in humans.

Given the unpredictability of filovirus outbreaks, the design and execution of clinical efficacy trials for vaccines and postexposure therapeutics in humans remains challenging and is inherently opportunistic. Despite the devastating social and economic impacts of the 2013-2016 West African EBOV epidemic, its unprecedented scale, both in size and duration, afforded the opportunity to assess the effectiveness of preexposure and postexposure medical countermeasures during a natural outbreak. The recombinant vesicular stomatitis virus vaccine (rVSV-ΔG-ZEBOV-GP, ERVEBO) demonstrated complete protection from new infections when administered during an open-label phase 3 ring vaccination trial[24], which led to its eventual approval as the first licensed vaccine for a filovirus[25]. A separate trial conducted toward the end of the epidemic demonstrated that ZMapp, a cocktail of three EBOV glycoprotein (GP)-specific mAbs[19], was 91.2% more likely to have prevented Ebola virus disease (EVD)-associated mortality than standard supportive care alone, although this fell short of the pre-specified study goal of 97.5%[26]. However, the PALM trial, conducted during the 2018-2020 EBOV outbreak in DRC, found that two other mAb products, mAb114 and REGN-EB3, were statistically superior to both ZMapp and remdesivir at reducing mortality from EVD[27]. Clinical trials assessing postexposure therapies, particularly with regard to highly virulent pathogens such as EBOV, are further complicated compared to vaccine studies in that patients are typically already symptomatic and may be in varying phases of disease severity upon enrollment. Moreover, preclinical studies in NHPs, while benefiting from being more tightly controlled internally, are typically conducted by multiple independent laboratories at different facilities, utilizing different protocols, virus stocks, challenge doses/routes, and/or NHP species. Thus, with regard to postexposure treatments for EVD, it remains unclear how effective relative to each other these interventions are when given at advanced stages of illness.

Here, we assessed the therapeutic efficacy of remdesivir, mAb114, REGN-EB3, and ZMapp in a uniformly lethal rhesus monkey model of EVD. Importantly, the macaques were infected with the same low passage EBOV seed stock by the same route and dose. Treatments were all initiated beginning on day 5 after challenge by intravenous (i.v.) administration performed at the same Biosafety Level (BSL)-4 facility by the same staff in order to best compare the efficacy of the four different treatments. The inability of any of the four therapies to completely protect animals suggests alternate strategies, such as combining therapeutics, as a potential avenue of treatment.

Results

NHP challenge with EBOV and efficacy of postexposure prophylaxis

We performed a series of challenge and treatment experiments in rhesus macaques utilizing the same seed stock and target dose of the Kikwit variant of EBOV inoculated via the intramuscular (i.m.) route. In an initial study, 10 macaques were challenged with a 1000 PFU target dose of EBOV. Beginning 5 days post EBOV infection (DPI), one group of animals ($n = 4$) were treated i.v. with 50 mg/kg of plant-derived ZMapp (ZMP), a second group ($n = 4$) were treated i.v. with 50 mg/kg of Chinese hamster ovary (CHO)-derived ZMapp (ZMC), and two EBOV-positive control animals were treated with vehicle only. All 10 animals received additional treatments on days 8 and 11. All animals showed clinical signs and/or serum biochemical markers consistent with the onset of clinical disease at the time that treatment was initiated (Supplementary Table 1), which included a combination of some or all of the following: fever, decreased appetite/anorexia, depression, petechial rash, lymphocytopenia, thrombocytopenia, monocytopenia, generalized granulocytosis (defined as an increase in the total number of granulocytes [e.g., neutrophils, eosinophils, basophils] over baseline values), hypoamylasemia, hypoalbuminemia, and elevated levels of markers of hepatic/renal injury (e.g., AST, ALT, BUN) and systemic inflammation (CRP). Deviations in these and other markers (e.g., CRE, GGT, ALP) progressed or persisted in animals which eventually succumbed to disease, whereas animals that survived challenge saw a gradual decrease or elimination in clinical signs and biochemical markers of disease. Three of four animals in the ZMP-treated group succumbed to lethal disease 7, 8, and 8 DPI (mean time to death [MTD] = 7.7 ± 0.5 DPI), while one survived to the predetermined study endpoint (28 DPI). Two of four animals in the ZMC-treated group succumbed to lethal disease on 10 and 11 DPI (MTD = 10.5 ± 0.5 DPI), while two animals survived to the study endpoint (28 DPI). The two vehicle-treated control animals both succumbed 6 DPI (MTD = 6.0 ± 0.0 DPI).

In a second study, 11 rhesus monkeys were challenged i.m. with a 1000 PFU target dose of EBOV. Beginning 5 days after EBOV exposure, five animals were treated i.v. with a single dose of 150 mg/kg of REGN-EB3, five macaques were treated i.v. with a loading dose of 10 mg/kg of remdesivir followed by daily maintenance doses from days 6–17 of 5 mg/kg of remdesivir, while the EBOV-positive control animal was not treated. At the time that treatment was initiated, all animals displayed a combination of clinical signs and/or serum biochemical markers of disease consistent those observed in the first study (Supplementary Tables 2, 3). Three of five animals in the remdesivir-treated group succumbed to lethal disease 5, 6, and 9 DPI (MTD = 6.7 ± 1.7 DPI), while two remdesivir-treated animals survived to the study endpoint (35 DPI). Similarly, three of five animals in the REGN-EB3-treated group succumbed to lethal disease 6, 8, and 8 DPI (MTD = 7.3 ± 0.9 DPI), while the single positive control animal succumbed 6 DPI.

In a final study, six rhesus monkeys were challenged i.m. with a 1000 PFU target dose of EBOV. At 5 DPI, five animals were treated i.v. with a single dose of 50 mg/kg of mAb114, while a single EBOV-positive control animal was not treated. At the time treatment was initiated, all animals exhibited some or all clinical signs and/or biochemical markers of disease as those observed in the previous two studies (Supplementary Table 4). Three of five animals treated with mAb114 succumbed to lethal disease 8, 9, and 14 DPI (MTD = 10.3 ± 2.6 DPI), while two animals survived to the study endpoint (35 DPI). The positive control animal succumbed to lethal disease 5 DPI.

To compare the therapeutic efficacy of each treatment regimen in preventing lethal disease, we compared the Kaplan-Meier survival curves as well as the proportional survival of animals from each group (Fig. 1a). To facilitate comparison, survival data from 14 historical positive control rhesus macaques from previous studies[13,28,29] (MTD = 7.4 ± 1.0 DPI) challenged with the identical seed stock, dose, and route were pooled with the four in-study controls from the current studies (MTD = 5.8 ± 0.4 DPI) for a total of 18 positive control animals (MTD = 7.0 ± 1.2 DPI). As there was no statistical difference in the survival between the ZMP and ZMC treated groups ($p = 0.234$, Mantel-Cox log-rank test; $p = 0.999$, Fisher's exact test), for comparison between treatment arms, all ZMapp-treated animals were grouped together.

https://doi.org/10.1038/s41467-025-59168-5

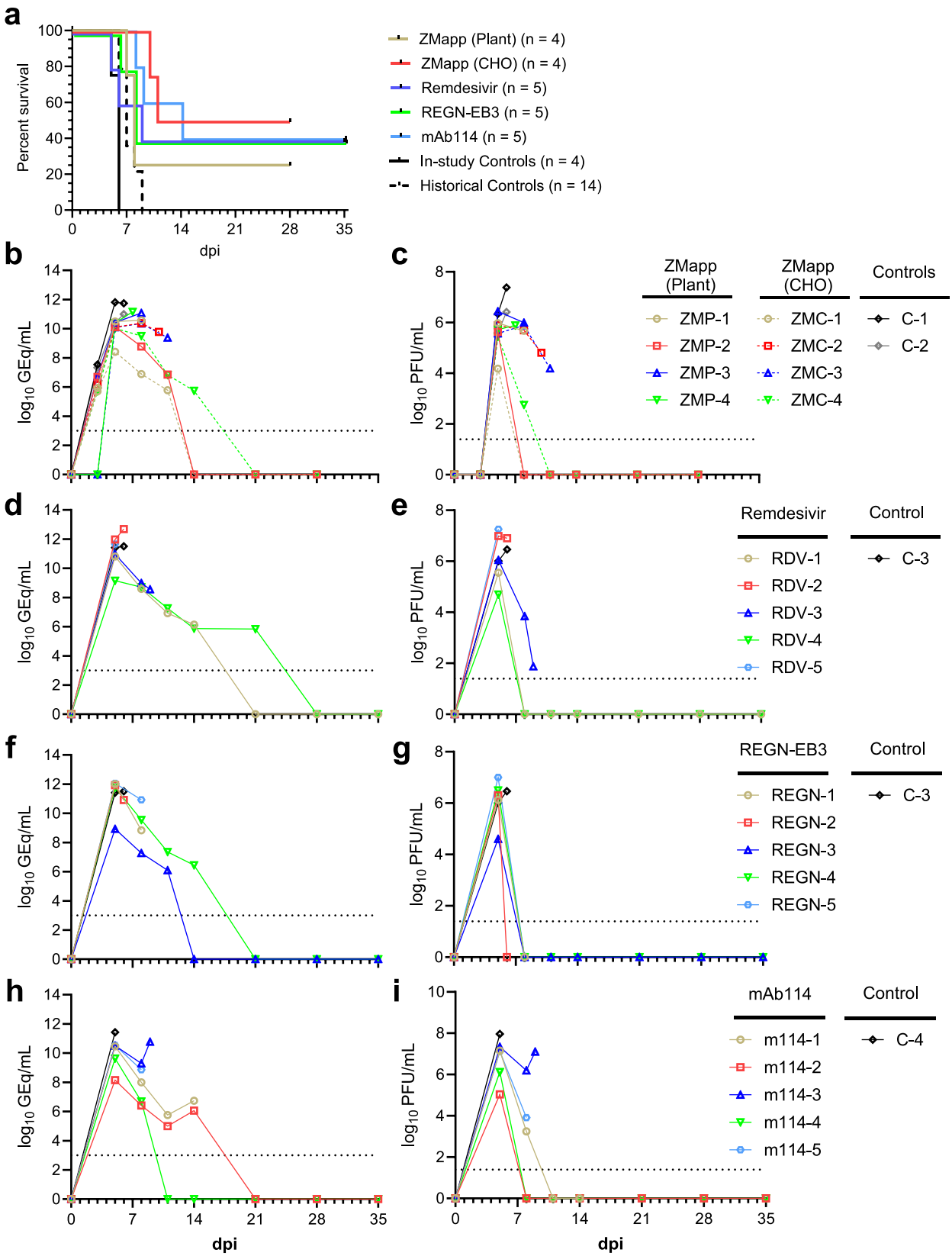

There was a statistical difference in the survival curves between the ZMapp-treated and the mAb114-treated cohorts versus the control cohort (multiplicity-corrected $p = 0.003$ and $p = 0.006$, respectively; Mantel-Cox log-rank test, Holm-Šídák correction for multiple comparisons). Statistically significant differences in proportional survival were observed for all four treatment cohorts compared to the control cohort (multiplicity-corrected $p = 0.0395$ for all comparisons; Fisher's exact test, Hochberg correction for multiple comparisons).

To determine whether individual survival outcome was associated with serum biomarkers indicative of more advanced disease, we compared the fold change difference at treatment initiation (5 DPI) of ALT, AST, and CRE to baseline (day of challenge) between animals that

Fig. 1 | Survival analysis and quantification of viral burden in rhesus macaques infected with EBOV and treated beginning 5 DPI with ZMapp, remdesivir, REGN-EB3, or mAb114. a Kaplan–Meier survival curves of macaques treated with ZMapp, remdesivir, REGN-EB3, or mAb114 beginning 5 DPI. Curves for ZMP and ZMC-treated animals and in-study control and historical control animals are shown separately; however, for statistical comparison between cohorts, all ZMapp treated animals were grouped together, and the in-study control animals were grouped with historical control animals. Statistical significance was determined using the Mantel-Cox log-rank test. **b** Viral load as measured by RT-qPCR amplification of EBOV genomic RNA (vRNA) in whole blood from ZMapp-treated animals and untreated in-study controls animals. **c** Plaque titration of circulating infectious virus from the plasma from ZMapp-treated animals and untreated in-study controls animals. **d** Viral load as measured by RT-qPCR amplification of EBOV vRNA in whole blood from remdesivir-treated animals and the untreated in-study control animal. **e** Plaque titration of circulating infectious virus from the plasma from remdesivir-treated animals and the untreated in-study control animal. **f** Viral load as measured by RT-qPCR amplification of EBOV vRNA in whole blood from REGN-EB3-treated animals and the untreated in-study control animal. **g** Plaque titration of circulating infectious virus from the plasma from REGN-EB3-treated animals and the untreated in-study control animal. **h** Viral load as measured by RT-qPCR amplification of EBOV vRNA in whole blood from mAb114-treated animals and the untreated in-study control animal. **i** Plaque titration of circulating infectious virus from the plasma from mAb114-treated animals and the untreated in-study control animal. Note that for (**d**–**g**) the untreated control animal (C-3) was shared between treatment groups. For (**b**–**i**) individual data points represent the mean of two technical replicates. Dashed horizontal lines indicate the lower limit of quantitation (LLOQ) for the assay (1000 GEq/mL for RT-qPCR; 25 PFU/mL for plaque titration, where GEq = genome equivalents). To fit on a log scale axis, zero values (below LLOQ) are plotted as "1" (10^0).

went on to survive challenge versus those that succumbed to disease. Animals were grouped by clinical outcome irrespective of treatment cohort. Animals which survived had significantly lower levels of ALT, AST and CRE (Supplementary Fig. 1a–c, $p = 0.047$, $p = 0.033$ and $p = 0.020$, respectively; Mann–Whitney *U*-test). However, the association between these markers and death was dependent on one (for ALT), two (for AST) or three (for CRE) individuals with exceptionally high values.

Quantification of viral burden in blood and tissues by RT-qPCR and plaque titration

For all animals across all cohorts, the kinetics of viral replication were assessed by RT-qPCR detection of EBOV genomic RNA (vRNA) in whole blood and plaque titration of infectious EBOV from plasma, respectively. All animals had detectable vRNA and circulating infectious virus at the time treatment was initiated (5 DPI) (Figs. 1b–i, 2a, b). As with the survival analysis, data from the two ZMapp treated cohorts was pooled for statistical comparison. There was no significant difference in vRNA abundance ($p \geq 0.085$ for all comparisons, non-parametric Dunn's test for multiple-comparisons) nor circulating viremia ($p \geq 0.383$ for all comparisons, non-parametric Dunn's test for multiple-comparisons) between treatment cohorts or to the control cohort at 5 DPI (Fig. 2a, b). Across all treatment groups, surviving animals experienced a reduction of both vRNA and infectious EBOV to below the detection threshold (Fig. 1b–i); however, due to the low number of surviving animals from each treatment group, statistical comparisons of peak viral burden or the day of last detectable vRNA/infectious virus between groups were not performed. Across treatment groups, all surviving animals were free of detectable vRNA in whole blood after 14 DPI, except for subject RDV-4 from the remdesivir cohort, which was positive for EBOV vRNA at 21 DPI (Fig. 1d). Only a single surviving animal (ZMC-4) had detectable infectious virus at 8 DPI (Fig. 1c), which was low in titer (2.8 $\log_{10}$ PFU/mL) and undetectable by 11 DPI, indicating that irrespective of treatment regimen, surviving animals uniformly experienced a rapid reduction in viremia.

To determine whether the individual viral burden at the time treatment was initiated affected the clinical outcome of infection, we compared the vRNA abundance and circulating viremia at the time of treatment initiation (5 DPI) between animals that went on to survive challenge versus those that succumbed to disease. Animals were grouped by clinical outcome irrespective of treatment cohort. Animals which survived had significantly lower levels of circulating vRNA ($p = 0.005$; Mann–Whitney *U*-test) and infectious EBOV ($p = 0.001$; Mann–Whitney *U*-test) at the time of treatment initiation compared to those that did not survive challenge (Fig. 2c, d).

Tissues were harvested at necropsy from all animals following euthanasia due to advanced disease or at the pre-determined study endpoint and assayed for the presence of EBOV vRNA by RT-qPCR (Fig. 3a–d). EBOV vRNA abundance was relatively consistent in all tissues analyzed from survivors across all treatment groups, ranging from ~ 6 $\log_{10}$ GEq/g – 8 $\log_{10}$ GEq/g tissue. EBOV vRNA abundance was ~2–4 $\log_{10}$ greater in most tissues from treated animals that succumbed to disease or in-study positive control animals compared to survivors, except for the eyes, which had similar levels of EBOV vRNA regardless of treatment group or clinical outcome. Most though not all surviving animals had modest levels (~6 $\log_{10}$ GEq/g tissue) of EBOV vRNA in CNS tissue (e.g., brain frontal cortex, brain stem, cervical spinal column).

Gross lesions and histopathology

Necropsies were performed on all animals from all studies by a board-certified veterinary pathologist, and animals were assessed both for gross lesions as well as by histopathological analysis. Across all treatment studies, lesions and immunolabeling in the representative tissues were consistent with EVD in NHPs that succumbed to disease. Gross findings for the NHPs that succumbed during the acute phase of the disease included some or all of the following: reticulated hepatic pallor, lymphadenomegaly, splenomegaly, adrenomegaly, petechial rash, hemorrhagic cystitis, hemorrhagic enteritis, hemorrhagic orchitis, and ascites.

In the ZMapp treatment study, no appreciable gross lesions were noted in ZMP-2 and ZMC-1; however, mild lymphadenomegaly was noted in subject ZMC-4. Lesions and immunolabeling in the representative tissues were consistent with EVD in NHPs that succumbed to disease (ZMP-1, ZMP-3, ZMP-4, ZMC-2, ZMC-3, C-1, and C-2). Lymphohistiocytic perivascular cuffs in the neuroparenchyma and within the choroid plexus lacking immunolabeling were noted in one treated NHP (ZMC-4) that survived to the study endpoint (Supplementary Fig. 2l, l inset). The two remaining survivors (ZMP-2 and ZMC-1) lacked lesions and immunolabeling. Lymphoid lesions consistent with EVD included sinus histiocytosis, fibrin deposition, and necrosis of germinal centers (Supplementary Fig. 2d, e). Positive immunohistochemistry (IHC) for EBOV antigen was noted in mononuclear cells throughout the lymphoid tissues (Supplementary Fig. 2d inset, e inset, j). Multifocal necrotizing hepatitis was noted in NHPs that succumbed to disease. Positive IHC was noted in Kupffer cells, mononuclear cells, hepatic sinusoidal lining cells, and rarely, hepatocytes (Supplementary Fig. 2a, b). Lesions associated with the urogenital tissue included lymphohistiocytic interstitial inflammatory infiltrates of the urinary bladder and epididymis, testis, and prostate. Positive IHC was noted in endothelium and mononuclear cells within the interstitium of the kidney, urinary bladder, epididymis, testis (Supplementary Fig. 2g), prostate, uterus and thecal cells of the ovary (Supplementary Fig. 2h). In pulmonary tissues, alveolar septae were thickened with lymphohistiocytic infiltrates and minimal flooding of alveolar spaces with edema and increased numbers of alveolar macrophages. IHC positivity for anti-EBOV antigen was noted in the alveolar septum, alveolar macrophages and occasionally, the endothelium (Supplementary

https://doi.org/10.1038/s41467-025-59168-5

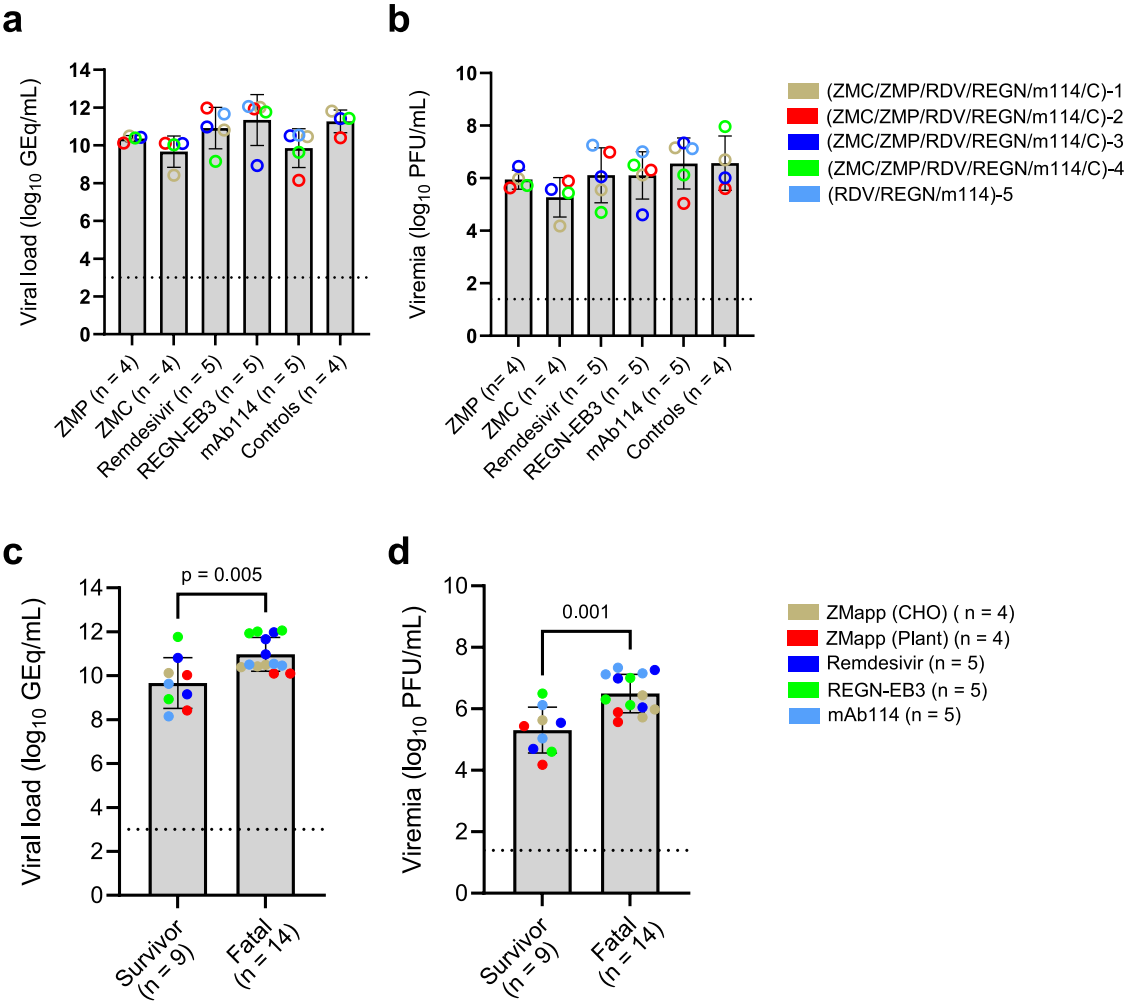

Fig. 2 | Comparisons of viral burden at treatment initiation (5 DPI) by treatment cohort and clinical outcome. EBOV vRNA abundance and circulating viremia was assessed at the time of treatment initiation (5 DPI) for each animal in each treatment cohort. **a**, **b** Comparison of EBOV vRNA abundance (**a**) and circulating live virus (**b**) at 5 DPI by treatment cohort. **c**, **d** Comparison of EBOV vRNA abundance (**c**) and circulating live virus at 5 DPI (**d**) by clinical outcome ("survivor" or "fatal"). For all panels, bars represent the geometric mean ± geometric SD for each group. For (**a**, **b**) individual animals are represented by color-coded symbols within bars. For (**a**, **b**) statistical comparison was performed by non-parametric ANOVA (Kruskal-Wallis test) followed by Dunn's post-hoc test for multiple comparisons. For (**c**, **d**) significance was determined by non-parametric Mann–Whitney *U*-test. All reported *p*-values are two-tailed. For all panels, individual data points represent the mean of two technical replicates. Dashed horizontal lines indicate the lower limit of quantitation (LLOQ) for the assay (1000 GEq/mL for RT-qPCR; 25 PFU/mL for plaque titration, where GEq = genome equivalents).

Fig. 2k). Adrenalitis was noted on H&E with associated IHC positivity of scattered mononuclear cells and clusters of cortical cells.

In the remdesivir and REGN-EB3 treatment studies, no appreciable gross lesions were noted in the two surviving NHPs treated with REGN-EB3 (REGN-3 and REGN-4); however, mild lymphadenomegaly was noted in the two surviving animals (RDV-1 and RDV-4) treated with remdesivir. In both treatment cohorts, lesions and immunolabeling in the representative tissues were consistent with EVD in NHPs that succumbed to disease (RDV-2, RDV-3, RDV-5, REGN-1, REGN-2, REGN-5, and C-3). Marked locally extensive lymphohistiocytic meningitis with focal extension into the underlying neuroparenchyma, perivascular cuffing, and focal IHC labeling of cells within the neuroparenchyma was noted in subject REGN-4, which survived challenge (Supplementary Fig. 3v–x). No appreciable lesions or immunolabeling of the neuroparenchyma were noted in remaining treatment survivors (Supplementary Fig. 3u). Ocular inflammation was noted in one remdesivir treatment survivor (RDV-1). Lymphohistiocytic inflammation was noted in the anterior uvea (iris, ciliary body), trabecular meshwork, free within the posterior chamber, and along the ora serrata within the vitreous chamber. Rarely, individual histiocytes within the ciliary body were IHC positive; however, they lacked ISH labeling (Supplementary Fig. 3i). Minimal lymphohistiocytic inflammation with IHC labeling was noted within the ciliary body of the control animal (C-3) and one remdesivir treated NHP (RDV-2) that succumbed to disease (Supplementary Fig. 3d, h). No appreciable lesions or IHC labeling were noted in the ocular tissues of the remaining NHPs that succumbed to disease (RDV-3, RDV-5, REGN-1, REGN-2 [Supplementary Fig. 3p], REGN-5) and the remaining treatment survivors (RDV-4, REGN-3, REGN-4 [Supplementary Fig. 3t]). Lymphoid lesions consistent with EVD included sinus histiocytosis, fibrin deposition, and necrosis of germinal centers (Supplementary Fig. 3b, f, n). Positive IHC for anti-EBOV antigen was noted in mononuclear cells throughout the lymphoid tissues (Supplementary Fig. 3c, g, o). Multifocal necrotizing hepatitis was noted in NHPs that succumbed to disease. Positive IHC was noted in Kupffer cells, mononuclear cells, hepatic sinusoidal lining cells, and rarely, hepatocytes (Supplementary Fig. 3a, e, m).

In the mAb114 treatment study, gross lesions for subject m114-1, which exhibited a delayed time to death (DTTD) of 14 DPI, included unilateral hypopyon, uveitis, and conjunctivitis (Supplementary Fig. 4k), bilateral blepharitis, multifocal hepatitis with white, flat

https://doi.org/10.1038/s41467-025-59168-5

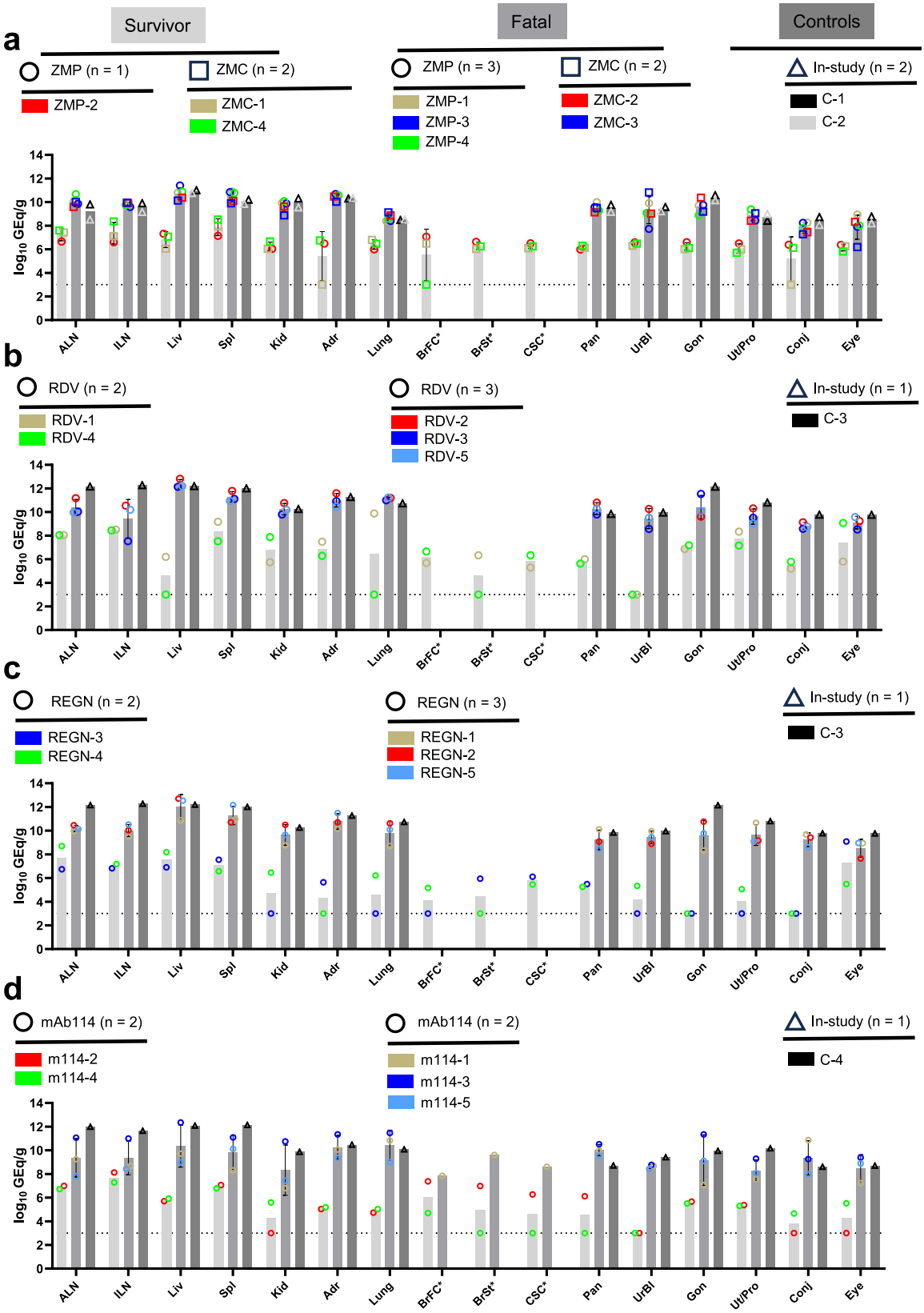

reticulation that was superimposed with white, raised, pinpoint randomly distributed foci, and lymphadenomegaly. No appreciable gross lesions were noted in surviving NHPs (m114-2 and m114-4). Lesions and immunolabeling in representative tissues were consistent with EVD in NHPs that succumbed to acute disease (m114-3, m114-5, C-4). Subject m114-1, which succumbed 14 DPI, had lesions and positive immunolabeling; however, the inflammatory infiltrate had a prominent neutrophilic component in multiple organs, including the liver, eye and brain. Lymphoid lesions consistent with EVD included sinus histiocytosis, fibrin deposition, and necrosis of germinal centers (Supplementary Fig. 4d). Positive IHC for anti-EBOV antigen was noted in mononuclear cells throughout the lymphoid tissues (Supplementary

Fig. 3 | Viral load in tissues from rhesus macaques infected with EBOV and treated beginning 5 DPI with ZMapp, remdesivir, REGN-EB3, or mAb114. The viral load in selected tissues sampled at necropsy was assessed by RT-qPCR amplification of EBOV vRNA. For each treatment group, treated animals were grouped by clinical outcome ("survivor" or "fatal"), while the in-study control(s) were plotted separately. **a** Tissue viral load in animals from the ZMapp treatment study (**b**) Tissue viral load in animals from the remdesivir treatment study. **c** Tissue viral load in animals from the REGN-EB3 treatment study. **d** Tissue viral load in animals from the mAb114 treatment study. Bars represent the geometric mean ± geometric SD for each group. Individual animals are represented by color-coded symbols within bars. For all panels, individual data points represent the mean of two technical replicates. Dashed horizontal lines indicate the lower limit of quantitation (LLOQ) for the assay (1000 GEq/g tissue, where GEq genome equivalents). Values below the LLOQ are plotted as 999 GEq/g tissue. Missing values indicate the given tissue was not assessed for that animal. Tissues with asterisks were only assessed for surviving animals, except in (**d**), where tissues were screened for a single animal (m114-1) with a delayed time to death (DDTD) of 14 DPI. Due to the small sample sizes in each cohort, statistical analysis was not performed. Abbreviations for tissues: ALN axillary lymph node, ILN inguinal lymph node, Liv liver, Spl spleen, Kid kidney, Adr adrenal gland, BrFr brain frontal cortex, BrSt brain stem, CSC cervical spinal cord, Pan pancreas, Uri urinary bladder, Gon gonad, Ut/Pro uterus/prostate, Conj conjunctiva.

Fig. 4d, inset). Multifocal necrotizing hepatitis was noted in NHPs that succumbed to disease. Positive IHC was noted in Kupffer cells, mononuclear cells, hepatic sinusoidal lining cells, and rarely, hepatocytes (Supplementary Fig. 4a). Few scattered mononuclear cells within the ciliary body of the eye and the conjunctiva were IHC positive (Supplementary Fig. 4g), as well as scattered interstitial cells of the pancreas. Lesions associated with the urogenital tissue included, lympohistiocytic interstitial inflammatory infiltrates of the kidney, urinary bladder, gonad, and prostate. Positive IHC was noted in endothelium and mononuclear cells within the interstitium of the kidney, urinary bladder, gonad, prostate or uterus. In pulmonary tissues, alveolar septae were thickened with lymphohistiocytic infiltrates and minimal flooding of alveolar spaces with edema and increased numbers of alveolar macrophages. IHC positivity for anti-EBOV antigen was noted in the alveolar septum, alveolar macrophages and occasionally, the endothelium. Adrenalitis was noted on H&E with associated IHC positivity of scattered mononuclear cells and clusters of cortical cells. Lesions in subject m114-1 with a DTTD included nodular pyogranulomatous inflammation of the liver (Supplementary Fig. 4b), marked pyogranulomatous anterior uveitis (Supplementary Fig. 4h, k, k inset), perivascular neutrophilic and lymphohistiocytic inflammation of the neuroparenchyma of the brain (Supplementary Fig. 4j, j inset, l,l inset), and neutrophilic and lymphohistiocytic vasculitis in the connective tissues surrounding the internal iliac lymph node, pancreas, urinary bladder, gonad, adrenal gland and conjunctiva/palpebrae. IHC positive cells were colocalized with inflammation. Subject m114-2, which survived challenge, had locally extensive neutrophilic and lymphohistiocytic, hemorrhagic meningoencephalitis (Supplementary Fig. 4m) with fibrinoid necrosis of vessel walls (Supplementary Fig. 4m, inset). Positive IHC labeling was associated with the inflammatory cells surrounding vessels of the meninges (Supplementary Fig. 4n) and colocalized with ISH labeling (Supplementary Fig. 4o, o inset). No appreciable lesions or immunolabeling were noted in the other examined tissues of m114-2 and in all tissues of the remaining survivor (m114-4).

In summary, surviving animals from all treatment cohorts were generally free of gross lesions indicative of EVD at the study endpoint (excepting mild lymphadenomegaly in three subjects); while animals that succumbed to disease displayed gross lesions comparable to positive control animals. In addition, the limited immunolabeling observed CNS or ocular tissue from three surviving subjects from the remdesivir, REGN-EB3, and mAb114 treatment cohorts did not appear to be treatment specific, although any statistical analysis is not possible due to the small number of affected subjects.

Variant analysis

To investigate whether any mutations emerged that might facilitate antibody escape, we performed deep sequencing of tissue RNA samples from each experimental group for variant analysis. Representative spleen or lung samples were selected based on high viral loads as determined by RT-qPCR. The samples included: Control (C-1 spleen, C-2 spleen, C-3 spleen, C-4 spleen), ZMP (ZMP-1 spleen, ZMP-3 spleen, ZMP-4 spleen), ZMC (ZMC-2 spleen, ZMC-3 spleen), RDV (RDV-2 spleen, RDV-3 spleen, RDV-5 spleen), REGN (REGN-1 spleen, REGN-2 spleen, REGN-5 spleen), and m114 (m114-1 lung, m114-3 spleen, m114-5 spleen). A schematic illustrating the positions of these mutations is presented in Fig. 4.

Mutation analysis was restricted to variants representing 10% or more of the viral population (Supplementary Data 1). The highest frequency variants predominantly arose in the mAb114 single monoclonal antibody group, with three non-synonymous mutations, A6387G:Asn117Asp and C6469T:Thr144Met (both from subject m114-3) and G6390A:Gly118Arg from subject m114-5, and two synonymous mutations, A7787:Ser583 and G7816A:Leu593, both from subject m114-1. The non-synonymous mutations were located in the receptor binding domain (RBD) of GP1 and were completely absent from LoFreq analysis of the challenge inoculum, while the synonymous mutations were found in the GP2 heptad repeat 1 domain and were present in low frequency in the challenge inoculum (<1%). Of note, none of the variants sequenced from the m114-treatment group were found in more than one animal.

In contrast, no mutations were observed in the REGN triple-antibody cocktail group, and only one mutation was identified in the spleen from subject ZMC-2 (CT8037C: indel), which is located in the GP2 transmembrane region. No significant variants were detected in the positive control group. These results indicate that single monoclonal antibodies may be more susceptible to antibody escape compared to antibody cocktails.

Discussion

The increased incidence of natural outbreaks caused by EBOV and other filoviruses poses a significant threat to human health globally. The large-scale emergence/re-emergence of EBOV and other highly pathogenic viruses into human populations should be expected to increase in frequency, as a number of anthropogenic factors such as deforestation, land use, urbanization, and globalization facilitate "spillover" events and widespread human-to-human transmission[30]. In addition, owing to their potential as an agent of biowarfare/bioterrorism, EBOV and Marburg virus (MARV) are both listed as Tier 1 select agent risk group 4 pathogens[31,32], emphasizing the need for highly efficacious vaccines and post-exposure prophylaxes to mitigate disease-associated morbidity and mortality.

While the severity of disease caused by EBOV and other filoviruses underscores the critical need for highly effective medical countermeasures, the unpredictable nature of outbreaks has proven to be a substantial challenge in assessing the efficacy of vaccines and therapeutics through well-controlled human clinical trials[33], further compounded by the sociopolitics, cultural climate, and poor medical infrastructure in some endemic regions[34]. Despite these formidable hurdles, clinical trials conducted during the 2013-2016 West African epidemic and 2018-2020 DRC EBOV outbreak resulted in the eventual licensure of an EBOV vaccine and two mAb-based treatments for human use[10,11,25], representing watershed moments in the mitigation of future outbreaks.

ZMapp was the first EBOV postexposure therapeutic assessed for efficacy in humans, during a trial in the later part of the 2013-2016 West

https://doi.org/10.1038/s41467-025-59168-5

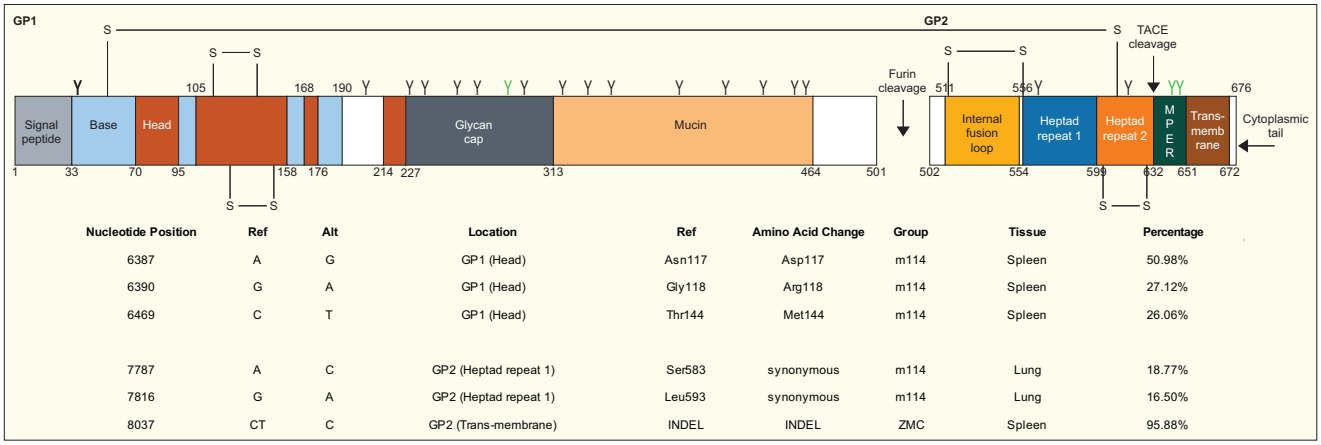

Nucleotide Position	Ref	Alt	Location	Ref	Amino Acid Change	Group	Tissue	Percentage
6387	A	G	GP1 (Head)	Asn117	Asp117	m114	Spleen	50.98%
6390	G	A	GP1 (Head)	Gly118	Arg118	m114	Spleen	27.12%
6469	C	T	GP1 (Head)	Thr144	Met144	m114	Spleen	26.06%
7787	A	C	GP2 (Heptad repeat 1)	Ser583	synonymous	m114	Lung	18.77%
7816	G	A	GP2 (Heptad repeat 1)	Leu593	synonymous	m114	Lung	16.50%
8037	CT	C	GP2 (Trans-membrane)	INDEL	INDEL	ZMC	Spleen	95.88%

Fig. 4 | Variant analysis of treated NHP tissues following EBOV exposure. The full-length glycoprotein (GP) is translated as a precursor of ~670 amino acids and is cleaved by host furin into two disulfide-linked subunits, GP1 and GP2. GP1 is responsible for receptor binding and is composed of four domains: the base, head, glycan cap, and mucin-like domain (MLD). The GP2 subunit contains the fusion peptide and a TACE cleavage site that results in shed GP, which triggers immune activation and increases vascular permeability. The GP1 Base and Head are discontinuous. Each GP1 and GP2 domain is colored according to the description in the drawn-to-scale schematic. Representative spleen or lung RNA samples with high viral loads, as determined by RT-qPCR, were selected: Control (C-1 to C-4 spleens), ZMP (ZMP-1, ZMP-3, ZMP-4 spleens), ZMC (ZMC-2, ZMC-3 spleens), RDV (RDV-2, RDV-3, RDV-5 spleens), REGN (REGN-1, REGN-2, REGN-5 spleens), and m114 (m114-1 lung, m114-3, m114-5 spleens). Mutation analysis focused on variants representing 10% or more of the viral population that were absent or <1% in the LoFreq analysis of the UTMB EBOV-Kikwit seed stock. Black Y-shaped symbols designate predicted N-linked glycosylation sites, whereas green Y-shaped symbols designate predicted C-mannosylation sites. Abbreviations: MPER membrane-proximal external region.

African EBOV epidemic (PREVAIL II)[26]. Based on favorable, although statistically inconclusive results in mitigating EVD-associated mortality relative to supportive care alone, ZMapp was used as the control arm of a second clinical trial conducted during the 2018-2020 EBOV outbreak in DRC, which assessed the effectiveness of three other candidate treatments: remdesivir, mAb114, and REGN-EB3[27]. In this second trial, known as PALM (abbreviated from "pamoja tulinde maisha", Swahili for "together save lives"), patients were enrolled an average of 5.5 days after the appearance of EVD symptoms, with ~40% exhibiting a high viral load (defined in the study parameters as an RT-qPCR Ct of ≤22), and thus could be considered to be in an advanced stage of disease. The study concluded that mAb114 and REGN-EB3 were statistically superior to both ZMapp and remdesivir in mitigating EVD-associated mortality, to the extent that the ZMapp and remdesivir arms were terminated in favor of randomizing patients to only the mAb114 or REGN-EB3 arms. Although efforts were made to fairly randomize patients across the treatment arms, the study authors note that patients enrolled to receive ZMapp and remdesivir had higher mean baseline serum creatinine and aminotransferase (ALT, AST) levels than those receiving mAb114 or REGN-EB3[27]. Moreover, the mean time from randomization to administration of the first therapeutic infusion was longer in patients enrolled to receive ZMapp or remdesivir compared to those receiving mAb114 or REGN-EB3[27]. These caveats suggest that patients receiving either ZMapp or remdesivir may have been, on average, in a more advanced stage of EVD than those receiving mAb114 or REGN-EB3, and as the authors note, may have influenced the observed clinical outcomes. The PREVAIL II and PALM studies both illustrate the inherent difficulties in designing and conducting clinical efficacy trials for highly lethal pathogens, particularly in impoverished and/or otherwise unstable regions of the world.

Prior to the EBOV epidemic in West Africa, it was assumed that any licensure of a filovirus vaccine or therapeutic would be predicated on efficacy data generated from animal studies under the U.S. Food and Drug Administration's Animal Rule[35]. Indeed, this may still be the case for some filoviruses such as SUDV and MARV, which thus far, have occurred in humans with significantly lower frequency and magnitude than EBOV. As with any investigational drug, all four therapeutic agents in the PALM trial were initially assessed in animal models, including NHPs[17,19–22]. Efficacy studies for vaccines and therapeutics against filoviruses in NHPs typically use high titer virus dosages and inoculation routes (e.g., 1000 PFU via i.m. exposure) which produce, at least for EBOV and MARV, near uniform lethality in both rhesus and cynomolgus macaques[36]. While the disease observed in NHPs under these conditions faithfully reproduces EVD in humans, the disease course is accelerated, and animals typically succumb to disease 5-8 DPI[36]. However, in addition to inoculum dosage, route, viral isolate, and NHP species, other factors, such as the in vitro passage history of the challenge stock, may influence infection kinetics and lethality. Filoviruses typically undergo at least one passage in a permissive cell line (usually Vero E6) following initial isolation in order to produce large volumes of challenge inoculum to ensure uniformity across many experiments. However, challenge stocks are not generated by a central facility and then dispersed to other entities; rather, individual institutions typically receive a small volume of material to themselves amplify for experiments conducted at their facilities. Thus, the passage history of virus stocks, even derived from the same initial biological isolate, can vary between laboratories. The effect of in vitro serial passaging on RNA virus genomes has long been known[37]. In addition to stochastic effects which cannot be predicted, repeated passaging of EBOV and other members of *Orthoebolavirus*[38] in Vero E6 cells results in the rapid accumulation of virus genomes exhibiting an additional uridine residue at the *GP*-editing site[39]. The *GP*-editing site of wild-type EBOV genomes consists of a stretch of seven uridine residues (designated as 7U viruses), from which the primary translated protein is a non-structural secreted form of GP (sGP). The full-length structural GP is produced through transcriptional editing (the addition of an 8th uridine residue) and represents a minority product[40]. In viruses with an 8U genotype, only full-length GP and a second truncated product, small soluble (ss)GP[41], are produced. The potential immunomodulatory roles of sGP in infection and pathogenesis are reviewed in detail elsewhere[42]; however, germane to the discussion here is that all else being equal, virus stocks that are predominately composed of 8U genotypes exhibit a slower progression of disease in macaques with fewer or less dramatic shifts in clinical markers of infection[43,44], and may exhibit decreased lethality[44]. Perhaps the most difficult aspect to account for when comparing the results of NHP studies conducted by different entities in which survival is the primary endpoint is in the assessment of behavioral manifestations of clinical disease, which are

used to determine when euthanasia criteria has been met[36]. Research groups such as our own utilize institution-specific protocols for cage-side assessment of animal behavior, health, and disease progression, which is inherently subjective and reliant on the experience of those making clinical observations. These are some, but not all of the variables that may potentially explain variability in the results of studies from different laboratories.

The above points are relevant to the existing literature assessing the efficacy of ZMapp, remdesivir, mAb114, and REGN-EB3 in NHPs. Corti et al. reported complete protection (3/3) of rhesus macaques sequentially treated with 50 mg/kg of mAb114 on days 5, 6, and 7 post-challenge with the Kikwit isolate of EBOV; however, no information on the passage history or genotype diversity (specifically the percentage of 7U genotypes) was given[21]. Likewise, Warren et al. demonstrated protection in 6/6 rhesus macaques following treatment with remdesivir at either 10 mg per kg loading/3 mg per kg maintenance doses or 10 mg per kg loading/10 mg per kg maintenance doses for 12 consecutive days beginning 3 DPI[20]; however, no information on the passage history or 7U composition of the EBOV Kikwit stock used was provided. In a subsequent study, 4/6 rhesus macaques were protected from lethal disease through administration of remdesivir in a 10 mg per kg loading/5 mg per kg maintenance dose regimen for 12 consecutive days beginning 4 days post-exposure to 100 PFU of EBOV Kikwit via the aerosol route[23]. While no information regarding the passage history of the challenge stock was provided, the authors reported it to be 92.80% 7U. Pascal et al. rescued 8/9 rhesus macaques from lethal disease following administration of 100 or 150 mg/kg of REGN-EB3 at 5 DPI[22]. In this study, the passage 3 (from the original biological material) virus stock was deep sequenced and reported as 94.3% 7U. Finally, in the first study demonstrating complete rescue from advanced EBOV disease in NHPs, Qiu et al. protected 6/6 rhesus macaques from lethal disease from a passage 3 Kikwit variant vachallenge stock following three 50 mg/kg doses of ZMapp spaced 3 days apart beginning 5 DPI[19]. In this study, the 7U composition of the virus was reported as 80%; however, this was determined using low-resolution Sanger sequencing of individual viral plaques. The variability among the studies as discussed above should not be taken to be dismissive of the informative value of each study taken individually; but rather, illustrative of the challenges in performing direct comparisons between them.

To address these inconsistencies, we performed a series of therapeutic rescue experiments in rhesus macaques challenged with the EBOV Kikwit variant and subsequently treated with either ZMapp, remdesivir, REGN-EB3, or mAb114 initiated at a stage of advanced disease (5 DPI). Importantly, all of these studies utilized the same low-passage virus challenge stock (passage 2 from the original biological material) which was deep-sequenced and shown to be 100% 7U and inoculated at the same target dosage (1000 PFU) via the same route (i.m.) across all experiments. In addition, all three experiments were conducted by the same research personnel using identical protocols for animal procedures, assessment of animal health, disease progression, and euthanasia criteria. We found that all four treatment regimens significantly rescued macaques from lethal disease compared to untreated control animals, with the proportion of surviving animals across all treatment cohorts consistent at 37.5-40% (when the three ZMapp survivors were grouped together), similar to what was observed human patients with advanced EVD (RT-qPCR Ct value ≤ 22) treated with REGN-EB3 or mAb114 in the PALM trial[27]. Statistical comparisons of survival between treatment cohorts were not performed as an unfeasibly large number of animals per cohort (particularly in an ABSL-4 setting) would be required to achieve 80% power. However, our data suggests all four treatments demonstrate similar sub-optimal efficacy against a low-passage, high 7U content challenge virus in NHPs, contrasting with the results from previous studies[19–22]. All four treatments conferred similar benefits to survivors, e.g., a rapid reduction in viral burden and clinical markers of disease, though due to the small sample sizes statistical comparisons were not made for these parameters between treatment cohorts. Histopathologic abnormalities were observed in at least one survivor from each treatment group; however, due to the small sample size it is difficult to ascertain what association, if any, specific pathologies may have with individual treatment regimens. Furthermore, details of gross and histopathological findings from survivors, if any, were not consistently reported in the previous studies assessing each therapy individually. However, we have previously reported post-convalescent ocular morbidities (e.g., uveitis, conjunctivitis, periorbital edema, keratic precipitates) in rhesus macaques rescued from lethal SUDV infection treated with remdesivir and/or a pan-orthoebolavirus mAb cocktail MBP431, alone or in combination[16]; similar abnormalities were observed in subjects RDV-1 and m114-1, the former of which was treated with remdesivir and survived challenge, and the latter of which was treated with mAb114 and succumbed to disease 14 DPI. Thus, these pathologies appear to be related to viral invasion of immune-privileged tissue as opposed to treatment-specific outcomes. While surviving animals had moderate amounts of EBOV vRNA in most or all tissues analyzed at the study endpoint, most tissues from all survivors lacked IHC-reactivity for EBOV antigen. Interestingly, vRNA abundance in ocular tissue was similar in most animals across treatment groups regardless of clinical outcome, suggesting that none of these treatments were effective at preventing viral invasion of this immune privileged site. Residual vRNA in the absence of infectious virus has been documented by us in filovirus[45–47] and arenavirus[48,49] vaccine and treatment studies as well as others for a number of different virus infection models[50] and likely relates to ongoing immune clearance mechanisms (i.e., neutralizing antibodies, cellular immunity, etc.). Three animals which survived treatment exhibited IHC-reactivity in the CNS (subjects REGN-4 and m114-2) or ocular tissue (subject RDV-1); however, colocalization of EBOV antigen with vRNA was only observed in subject m114-2. While these animals were free of overt clinical signs of disease at the study endpoint (35 DPI), the potential for immune-privileged sites such as the eyes, CNS, and gonads to harbor replicating virus following convalescence is a concern given that EBOV may remain as a persistent and/or latent infection in these tissues and has resulted in the spontaneous re-initiation of subsequent outbreaks months or even years later[51–53].

As with human patients in the PALM trial[27], surviving macaques had a significantly lower viral burden (measured by both RT-qPCR of EBOV vRNA and plaque titration of circulating live virus) at the time treatment was initiated compared to animals which failed to be rescued from lethal disease. Elevated levels of serum ALT, AST, and CRE at the time of treatment initiation were weaker predictors of clinical outcome. The results of our studies allow for easier comparison of the therapeutic efficacy of these four EBOV treatments to one another than is afforded by individual NHP studies conducted by separate labs in different facilities and allow for more stringent control of variables than is possible in human clinical trials.

For ethical reasons, PALM did not include a control arm with no active therapeutic, so it did not show that remdesivir was ineffective at improving survival outcomes relative to standard of care alone. Therefore, the PALM trial should not be taken to suggest that, by extension, obeldesivir, an orally bioavailable isobutylester prodrug of the same parent nucleoside (GS-441524) as that contained in remdesivir itself has no value in treating EVD. Indeed, we have recently reported that once-daily oral treatment of cynomolgus monkeys with obeldesivir for 10 days beginning 24 h after SUDV exposure confers 100% protection against lethal infection[45]. Significant protection (80–100%) was also observed using the same treatment regimen in NHP models of EBOV[47] and MARV[46] infection. What is clear from both the PALM trial and the current study is that all of the therapeutics as assessed still allow for unacceptably high mortality rates, as even the

REGN-EB3 and mAb114 arms in the PALM trial experienced overall mortality rates of 33.5% (63.6% in patients with high viral loads) and 35.1% (69.9% in patients with high viral loads), respectively[27], compared to the overall 66% CFR for the outbreak[4].

We recently reported rescue from advanced disease in NHPs challenged with MARV or SUDV and then treated with a combination of remdesivir and a virus-specific antibody (in the MARV study) or a pan-orthoebolavirus antibody cocktail (in the SUDV study)[15,16]. In these studies, significant survival compared to untreated controls was conferred when the combination therapy was initiated as late as 6 DPI, beyond that of any other therapeutic for filoviruses in the published literature. In contrast, monotherapy with either remdesivir or the mAb(s) failed to rescue monkeys from lethal disease. Treatment with a small molecule inhibitor such as remdesivir in combination with a mAb or cocktail of mAbs is advantageous as protection likely stems from complementary but distinct mechanisms of action between remdesivir and antibody neutralization[15,16]. In addition, because of their very different physico-chemical properties, remdesivir and mAbs likely exhibit non-overlapping tissue distribution profiles, which might aid in limiting virus spread more broadly across different tissues. Moreover, concern exists for the possible generation of antibody escape mutants, particularly when a single antibody (as with mAb114) as opposed to a cocktail of mAbs (e.g., ZMapp or REGN-EB3) is used. Indeed, we identified a greater number of high-frequency (> 10%) variants in animals treated with mAb114, including three non-synonymous mutations within the highly-conserved RBD of GP1, which is targeted by mAb114[54], though we did not directly test whether these mutations conferred resistance to neutralization. Thus, combining remdesivir with a mAb or mAb-cocktail likely reduces the probability of antibody escape through the imposition of additional selective pressures. Therefore, it is likely that a similar combination of a small-molecule inhibitor and mAb or mAb-cocktail could further enhance survival outcomes to EBOV infection and should be an avenue of further research.

Methods

Challenge virus

Orthoebolavirus zairense (EBOV) isolate 199510621 (Kikwit variant) originated from a 65 year-old female patient who had died on 5 May 1995. The study challenge material was from the second Vero E6 passage of EBOV isolate 199510621. Briefly, the first passage at UTMB consisted of inoculating CDC 807223 (passage 1 of EBOV isolate 199510621) at a MOI of 0.001 onto Vero E6 cells. The cell culture fluids were subsequently harvested at day 10 post infection and stored at −80 °C as ~1 ml aliquots. Deep sequencing indicated the EBOV was 100% 7U (consecutive stretch of 7 uridines). No detectable mycoplasma or endotoxin levels were measured (<0.5 endotoxin units (EU)/ml).

Drug formulation

Remdesivir was synthesized at Gilead Sciences, Inc. The chemical identity and sample purity were established using NMR, HRMS, and HPLC analyses[20]. Small-molecule X-ray crystallographic coordinates and structure factor files have been deposited in the Cambridge Structural Database (http://www.ccdc.cam.ac.uk/); accession numbers have been supplied previously[20]. Remdesivir drug substance was solubilized in 12% sulfobutylether-β-cyclodextrin in water at pH 3.5 and matching vehicle solution was provided to UTMB for these studies. ZMapp was produced in or *N. benthamiana* or CHO cells as previously described[19,55]. REGN-EB3 was produced in CHO cells and purified as previously described[22]. Because we were unable to obtain mAb114 (Ansuvimab) from Ridgeback Biotherapeutics, research grade mAb114 manufactured by Mapp Biopharmaceutical (San Diego, CA) was used. Briefly, a dual-promoter plasmid containing expression cassettes for the heavy and light chains of mAb114 was used to transfect CHO-S cells and establish a stable cell line. The stable pool was scaled up in shake flasks and ~3 grams of antibody was purified using a Cytiva MabSelect SuRe LX Protein A affinity chromatography column on an AKTA pure 150 system. The eluate was immediately neutralized with 2 M Tris base to approximately pH 7. The neutralized eluate was diafiltered against the formulation buffer (20 mM histidine, 240 mM sucrose, pH 6.0) and concentrated to 30.7 mg/mL using a Sartorius 30 kD Hydrosart Sartocon Slice ECO cassette on a Sartorius SARTOFLOW Smart TFF system. Polysorbate-80 was added to 0.02% after the target mAb concentration was reached and the solution was filter sterilized.

Nonhuman primate challenge and treatment

Specific details of the three NHP challenge experiments are presented in the Results section. A total of 27 healthy, research-naïve, captive bred rhesus macaques (*Macaca mulatta*) ~2–16 years of age and weighing ~2.7–9.9 kg were obtained from several sources (Envigo, PreLabs, Tulane University Primate Center, Worldwide Primates). Assignment to a particular treatment group or control group was determined prior to challenge by randomization by Excel. Efforts were made to balance the sex distribution in each cohort (the sex of each individual is provided in Supplementary Tables S1–4); however, sex was not considered as part of the interpretation of results as it is not known or expected to influence the challenge outcome in either treated or control animals. Virus challenge was performed via intramuscular (i.m.) injection of a 1000 PFU target dose of EBOV in the left quadricep (actual doses of 1075, 888, and 1163 PFU for the first, second, and third studies, respectively). The duration of the ZMapp treatment study was 28 days, while the duration of the remdesivir, REGN-EB3, and mAb114 treatment studies was 35 days. For all studies, dosage and frequency regimens of each therapeutic were designed in congruence with those used in the PALM trial and/or published preclinical efficacy studies in NHPs[19–23,27]. Whole blood was collected and body mass and rectal temperature measured according to the following sampling schedule: day of challenge (0 DPI), 3 DPI (ZMapp study only), 5 DPI, 8 DPI, 11 DPI, 14 DPI, 21 DPI, 28 DPI, and 35 DPI (remdesivir, REGN-EB3, and mAb114 studies only), or at the time the animal met criteria for humane euthanasia. All 27 macaques were monitored daily and scored for disease progression with an internal EBOV humane endpoint scoring sheet approved by the UTMB Institutional Animal Care and Use Committee (IACUC) under UTMB number 2020063. UTMB facilities used in this work are accredited by the Association for Assessment and Accreditation of Laboratory Animal Care International and adhere to principles specified in the eighth edition of the Guide for the Care and Use of Laboratory Animals, National Research Council. The scoring changes measured from baseline included posture and activity level, attitude and behavior, food intake, respiration, and disease manifestations, such as visible rash, hemorrhage, ecchymosis, or flushed skin. A score of ≥9 indicated that an animal met the criteria for euthanasia.

Hematology and serum biochemistry

Total white blood cell counts, white blood cell differentials, red blood cell counts, platelet counts, hematocrit values, total hemoglobin concentrations, mean cell volumes, mean corpuscular volumes, and mean corpuscular hemoglobin concentrations were analyzed from blood collected in tubes containing EDTA using a Vetscan HM5 laser based hematologic analyzer (Zoetis). Serum samples were tested for concentrations of albumin, amylase, alanine aminotransferase (ALT), aspartate aminotransferase (AST), alkaline phosphatase (ALP), blood urea nitrogen (BUN), calcium, creatinine (CRE), C-reactive protein (CRP), gamma-glutamyltransferase (GGT), glucose, total protein, and uric acid by using a Piccolo point-of-care analyzer and Biochemistry Panel Plus analyzer discs (Abaxis).

Detection of viremia

RNA was isolated from whole blood utilizing the Viral RNA mini-kit (Qiagen) using 100 μl of blood added to 600 μl of the viral lysis buffer.

Primers and probe targeting the *VP30* gene of EBOV were used for real-time quantitative PCR (RT-qPCR) with the following primers and probe: Forward = 5′-AGC ACG ATC ATC ATC CAG AG-3′; Reverse = 5′-TAC AGT AGG AAC GCG CAC TT-3′; Probe = 6-carboxyfluorescein (FAM)-5′-CCG TCA ATC AAG GAG CGC CTC- 3′-6 carboxytetramethylrhodamine (TAMRA) (Life Technologies).Viral RNA was detected using the CFX96 detection system (Bio-Rad Laboratories, Hercules, CA) in one-step probe RT-qPCR kits (Qiagen) with the following cycle conditions: 50 °C for 10 min, 95 °C for 10 s, and 40 cycles of 95 °C for 10 s and 57 °C for 30 s. Threshold cycle (CT) values representing viral genomes were analyzed with CFX Manager software, and the data are shown as genome equivalents (GEq) per milliliter. To create the GEq standard, RNA from viral stocks was extracted, and the number of strain-specific genomes was calculated using Avogadro's number and the molecular weight of each viral genome.

Virus titration was performed for EBOV by plaque assay with Vero E6 cells (ATCC, CRL-1586) from all plasma samples as previously described[56,57]. Briefly, increasing 10-fold dilutions of the samples were adsorbed to Vero E6 monolayers in duplicate wells (200 μL) and overlaid with 0.8% agarose in 1 × Eagle's minimum essentials medium (EMEM) with 5% fetal bovine serum and 1% penicillin-streptomycin. After a 6 day incubation at 37 °C/5% CO2, neutral red stain was added, and plaques were counted after a 48 h incubation. The limit of detection for this assay was 25 PFU/mL

Histopathologic and immunohistochemical (IHC) analyses

Necropsy was performed on all subjects. Tissue samples from major organs were collected for histopathological and IHC examination, immersion fixed in 10% neutral buffered formalin and processed for histopathologic analysis as previously described[56,57]. Tissue sections were deparaffinized and rehydrated through xylene and graded ethanols. Slides went through heat antigen retrieval in a steamer at 95 °C for 20 min in Sigma Citrate Buffer, pH6.0, 10x (Sigma Aldrich, St. Louis, MO). The tissue sections were processed for IHC using the Thermo Autostainer 360 (ThermoFisher, Kalamazoo, MI). Specific anti-Ebola Zaire VP40 immunoreactivity was detected using an anti-Ebola Zaire VP40 primary antibody at a 1:4000 dilution for 60 min. Secondary antibody used was biotinylated goat anti-rabbit IgG (Vector Laboratories, Burlingame, CA, cat #BA-1000) at 1:200 for 30 min followed by Vector Streptavidin Alkaline Phosphatase at a dilution of 1:200 for 15 min (Vector Laboratories cat #SA-5100). Slides were developed with ImmPact Red Substrate Kit (Vector Laboratories cat #SK-5105) for 20 min and counterstained with hematoxylin for 30 sec.

EBOV RNA in situ hybridization (ISH) in formalin-fixed paraffin embedded (FFPE) tissues was performed using the RNAscope 2.5 high definition (HD) RED kit (Advanced Cell Diagnostics, Newark, CA) according to the manufacturer's instructions. 20 ZZ probe pairs targeting the genomic EBOV nucleoprotein (*NP*) gene were designed and synthesized by Advanced cell Diagnostics (cat #448581). After sectioning, deparaffinization with xylene, and graded ethanol washes and peroxidase blocking, the sections were heated in RNAscope Target Retrieval Reagent Buffer (Advanced Cell Diagnostics, cat #322000) for 45 min and then air-dried overnight. The sections were then digested with Protease IV (Advanced Cell Diagnostics, cat #322336) at 40 °C in the HybEZ oven (HybEZ, Advanced Cell Diagnostics, cat #321711) for 30 min. Sections were exposed to ISH target probe and incubated at 40 °C in the HybEZ oven for 2 h. After rinsing, the signal was amplified using the manufacturer provided pre-amplifier and amplifier conjugated to alkaline phosphatase and incubated with a red substrate-chromogen solution for 10 min, counterstained with hematoxylin, air-dried, and coverslipped.

Variant analysis

The tissue sample sequencing libraries were generated using the NEBNext Ultra II RNA Prep Kit (New England BioLabs, Inc.), following the manufacturer's instructions. Approximately 100 ng of RNA was fragmented for 15 min, followed by the synthesis of cDNA, end-repair, and adapter ligation. After five cycles of PCR, the libraries were analyzed using an Agilent Bioanalyzer and quantified through qPCR. The samples were pooled and sequenced using paired-end 75-base reads on the Illumina NextSeq 550 platform with the High-Output kit. Trimmomatic v0.36[58] was used to filter out low-quality base calls and remove adapter sequences. Assembly of the reads into contigs was performed using the de novo assembler ABySS[59], applying various sets of reads and kmer values ranging from 20–40. Contigs longer than 400 base pairs were compared to the NCBI nucleotide database using BLAST, resulting in a nearly complete EBOV-Kikwit viral contig. The remaining contigs aligned with host cell ribosomal RNA or mitochondrial sequences. Trimmed reads from each sample were aligned to the sample consensus sequence using BWA v0.7.17[60], and the assembly was verified through visualization with the Integrated Genomics Viewer[61]. Single nucleotide variants and insertion/deletion calls were generated by mapping the trimmed reads to the reference sequence using BWA. LoFreq version 2.1.3.1[62] was used for variant calling with the call and call-indels commands, following preprocessing with the LoFreq viterbi and indelqual commands to adjust read-end alignments and improve indel quality scores (see Supplementary Data 1). Variants were filtered at a threshold of 0.05%.

Statistical analysis

Details of specific statistical tests are provided in the Results and relevant figure captions. For statistical comparisons, survival data from four published[13,28,29] and ten unpublished historical control rhesus macaques challenged via the same route with the same virus stock and dose were added to the in-study control cohorts. All statistical analyses were performed in GraphPad Prism v10.4.1, except for the Hochberg correction for multiple comparisons, which was performed in R v.4.0.2[63] using the "p.adjust" function of the included stats v.4.0.2 package. Unless otherwise indicated, all reported *p*-values are two tailed and rounded to three decimal places.

Reporting summary

Further information on research design is available in the Nature Portfolio Reporting Summary linked to this article.

Data availability

Ebola virus is a BSL-4 and Tier 1 pathogen that requires permits from the US Centers for Disease Control and Prevention. All data generated or analyzed during this study are included in this published article (and its supplementary information files). The datasets generated during and/or analyzed during the current study are available from the corresponding author (TWG). Source Data are provided with this paper. The raw FASTQ files containing deep sequencing reads generated in this study have been deposited in the NCBI Sequence Read Archive (SRA) under accession code PRJNA1233197. Source data are provided with this paper.

References

1. Feldmann, H., Sanchez, A. & Geisbert, T. W. In *Fields Virology* (eds D. M. Knipe & P. M. Howley) 923–956 (Lippincott Williams & Wilkins, 2013).
2. Feldmann, H., Sprecher, A. & Geisbert, T. W. Ebola. *New Engl. J. Med.* **382**, 1832–1842 (2020).
3. World Health Organization. *Ebola: West Africa, March 2014-2016*. https://www.who.int/emergencies/situations/ebola-outbreak-2014-2016-West-Africa (2023).
4. World Health Organization. *Ebola: North Kivu/Ituri, Democratic Republic of the Congo, August 2018—June 2020*. https://www.who.int/emergencies/situations/Ebola-2019-drc (2024).
5. Dupuy, L. C. et al. Filoviruses: scientific gaps and prototype pathogen recommendation. *J. Infect. Dis.* **228**, S446–S459 (2023).

6. Emanuel, J., Marzi, A. & Feldmann, H. In *Advances in Virus Research* (eds Kielian M. Mettenleiter. T. C., & Roossinck. M. J.) 189–221 (Academic Press, 2018).
7. Cross, R. W., Mire, C. E., Feldmann, H. & Geisbert, T. W. Post-exposure treatments for Ebola and Marburg virus infections. *Nat. Rev. Drug Discov.* **17**, 413–434 (2018).
8. Woolsey, C. & Geisbert, T. W. Current state of Ebola virus vaccines: a snapshot. *PLoS Pathog.* **17**, e1010078 (2021).
9. Liu, C. H., Hu, Y. T., Wong, S. H. & Lin, L. T. Therapeutic strategies against ebola virus infection. *Viruses* **14**, 579 (2022).
10. Markham, A. REGN-EB3: First approval. *Drugs* **81**, 175–178 (2021).
11. Taki, E. et al. Ebanga: The most recent FDA-approved drug for treating Ebola. *Front. Pharmacol.* **14**, 1083429 (2023).
12. Mire, C. E. et al. Therapeutic treatment of Marburg and Ravn virus infection in nonhuman primates with a human monoclonal antibody. *Sci. Transl. Med.* **9**, eaai8711 (2017).
13. Bornholdt, Z. A. et al. A Two-antibody pan-ebolavirus cocktail confers broad therapeutic protection in ferrets and nonhuman primates. *Cell Host Microbe.* **25**, 49–58 e45 (2019).
14. Porter, D. P. et al. Remdesivir (GS-5734) is efficacious in cynomolgus macaques infected with marburg virus. *J. Infect. Dis.* **222**, 1894-1901 (2020).
15. Cross, R. W. et al. Combination therapy protects macaques against advanced Marburg virus disease. *Nat. Commun.* **12**, 1891 (2021).
16. Cross, R. W. et al. Combination therapy with remdesivir and monoclonal antibodies protects nonhuman primates against advanced Sudan virus disease. *JCI Insight* **7**, e159090 (2022).
17. Brannan, J. M. et al. Post-exposure immunotherapy for two ebolaviruses and Marburg virus in nonhuman primates. *Nat. Commun.* **10**, 105 (2019).
18. Kuang, E. et al. Reversion of Ebolavirus disease from a single intramuscular injection of a pan-ebolavirus immunotherapeutic. *Pathogens* **11**, 655 (2022).
19. Qiu, X. et al. Reversion of advanced Ebola virus disease in nonhuman primates with ZMapp. *Nature* **514**, 47–53 (2014).
20. Warren, T. K. et al. Therapeutic efficacy of the small molecule GS-5734 against Ebola virus in rhesus monkeys. *Nature* **531**, 381–385 (2016).
21. Corti, D. et al. Protective monotherapy against lethal Ebola virus infection by a potently neutralizing antibody. *Science* **351**, 1339–1342 (2016).
22. Pascal, K. E. et al. Development of clinical-stage human monoclonal antibodies that treat advanced Ebola virus disease in nonhuman primates. *J. Infect. Dis.* **218**, S612–S626 (2018).
23. Warren, T. K. et al. Remdesivir is efficacious in rhesus monkeys exposed to aerosolized Ebola virus. *Sci. Rep.* **11**, 19458 (2021).
24. Henao-Restrepo, A. M. et al. Efficacy and effectiveness of an rVSV-vectored vaccine in preventing Ebola virus disease: final results from the Guinea ring vaccination, open-label, cluster-randomised trial (Ebola Ca Suffit!). *Lancet* **389**, 505–518 (2017).
25. U.S. Food and Drug Administration. *First FDA-approved Vaccine For The Prevention Of Ebola Virus Disease, Marking A Critical Milestone In Public Health Preparedness And Response*. https://www.fda.gov/news-events/press-announcements/first-fda-approved-vaccine-prevention-ebola-virus-disease-marking-critical-milestone-public-health (2019).
26. Prevail II Writing Group. A randomized, controlled trial of ZMapp for Ebola virus infection. *N. Engl. J. Med.* **375**, 1448–1456 (2016).
27. Mulangu, S. et al. A randomized, controlled trial of Ebola virus disease therapeutics. *N. Engl. J. Med.* **381**, 2293–2303 (2019).
28. Gilchuk, P. et al. Pan-ebolavirus protective therapy by two multifunctional human antibodies. *Cell* **184**, 5593–5607 e5518 (2021).
29. Cross, R. W. et al. Prior vaccination with rVSV-ZEBOV does not interfere with but improves efficacy of postexposure antibody treatment. *Nat. Commun,* **11**, 3736 (2020).
30. Tazerji, S. S., Nardini, R., Safdar, M., Shehata, A. A. & Duarte, P. M. An overview of anthropogenic actions as drivers for emerging and re-emerging zoonotic diseases. *Pathogens* **11**, 1376 (2022).
31. Federal Select Agent Program. *Select Agents and Toxins List*. https://www.selectagents.gov/sat/list.htm (2024).
32. National Institute of Allergy and Infectious Diseases. *NIAID Emerging Infectious Diseases/Pathogens*. https://www.niaid.nih.gov/research/niaid-biodefense-pathogens (2024).
33. Sprecher, A. et al. Perspectives on advancing countermeasures for filovirus disease: report from a multisector meeting. *J. Infect. Dis.* **228**, S474–S478 (2023).
34. Nguyen, V.-K. An epidemic of suspicion—Ebola and violence in the DRC. *N. Engl. J. Med.* **380**, 1298–1299 (2019).
35. Allio, T. Product development under FDA's animal rule: understanding FDA's expectations and potential implications for traditional development programs. *Ther. Innov. Regul. Sci.* **50**, 660–670 (2016).
36. Geisbert, T. W., Strong, J. E. & Feldmann, H. Considerations in the use of nonhuman primate models of Ebola virus and Marburg virus infection. *J. Infect. Dis.* **212**, S91–S97 (2015).
37. Sobrino, F., Davila, M., Ortin, J. & Domingo, E. Multiple genetic variants arise in the course of replication of foot-and-mouth disease virus in cell culture. *Virology* **128**, 310–318 (1983).
38. Alfson, K. J. et al. Genetic changes at the glycoprotein editing site associated with serial passage of Sudan virus. *J. Infect. Dis.* **212**, S295–S304 (2015).
39. Volchkova, V. A., Dolnik, O., Martinez, M. J., Reynard, O. & Volchkov, V. E. Genomic RNA editing and its impact on Ebola virus adaptation during serial passages in cell culture and infection of guinea pigs. *J. Infect. Dis.* **204**, S941–S946 (2011).
40. Sanchez, A., Trappier, S. G., Mahy, B. W., Peters, C. J. & Nichol, S. T. The virion glycoproteins of Ebola viruses are encoded in two reading frames and are expressed through transcriptional editing. *Proc. Natl Acad. Sci. USA* **93**, 3602–3607 (1996).
41. Mehedi, M. et al. A new Ebola virus nonstructural glycoprotein expressed through RNA editing. *J. Virol.* **85**, 5406–5414 (2011).
42. Zhu, W., Banadyga, L., Emeterio, K., Wong, G. & Qiu, X. The roles of Ebola virus soluble glycoprotein in replication, pathogenesis, and countermeasure development. *Viruses* **11**, 999 (2019).
43. Trefry, J. C. et al. Ebola Virus infections in nonhuman primates are temporally influenced by glycoprotein poly-U editing site populations in the exposure material. *Viruses* **7**, 6739–6754 (2015).
44. Alfson, K. et al. Intramuscular exposure of macaca fascicularis to low doses of low passage- or cell culture-adapted Sudan virus or Ebola virus. *Viruses* **10**, 642 (2018).
45. Cross, R. W. et al. Oral administration of obeldesivir protects nonhuman primates against Sudan ebolavirus. *Science* **383**, eadk6176 (2024).
46. Cross, R. W. et al. Oral obeldesivir provides postexposure protection against Marburg virus in nonhuman primates. *Nat. Med.* **31**, 1303–1311 (2025).
47. Woolsey, C. et al. The oral drug obeldesivir protects nonhuman primates against lethal Ebola virus infection. *Sci. Adv.* **11**, eadw0659 (2025).
48. Mire, C. E. et al. Human-monoclonal-antibody therapy protects nonhuman primates against advanced Lassa fever. *Nat. Med.* **23**, 1146–1149 (2017).
49. Cross, R. W. et al. Quadrivalent VesiculoVax vaccine protects nonhuman primates from viral-induced hemorrhagic fever and death. *J. Clin. Invest.* **130**, 539–551 (2020).
50. Griffin, D. E. Why does viral RNA sometimes persist after recovery from acute infections? *PLoS Biol.* **20**, e3001687 (2022).
51. Diallo, B. et al. Resurgence of Ebola virus disease in Guinea linked to a survivor with virus persistence in seminal fluid for more than 500 days. *Clin. Infect. Dis.* **63**, 1353–1356 (2016).

52. Keita, A. K. et al. Resurgence of Ebola virus in 2021 in Guinea suggests a new paradigm for outbreaks. *Nature* **597**, 539–543 (2021).
53. Mbala-Kingebeni, P. et al. Ebola virus transmission initiated by relapse of systemic Ebola virus disease. *N. Engl. J. Med.* **384**, 1240–1247 (2021).
54. Misasi, J. et al. Structural and molecular basis for Ebola virus neutralization by protective human antibodies. *Science.* **351**, 1343–1346 (2016).
55. Pettit, D. K. et al. CHO cell production and sequence improvement in the 13C6FR1 anti-Ebola antibody. *Mabs.* **8**, 347–357 (2016).
56. Mire, C. E. et al. Single-dose attenuated Vesiculovax vaccines protect primates against Ebola Makona virus. *Nature* **520**, 688–691 (2015).
57. Thi, E. P. et al. Lipid nanoparticle siRNA treatment of Ebola-virus-Makona-infected nonhuman primates. *Nature.* **521**, 362–365 (2015).
58. Bolger, A. M., Lohse, M. & Usadel, B. Trimmomatic: A flexible trimmer for Illumina sequence data. *Bioinformatics.* **30**, 2114–2120 (2014).
59. Simpson, J. T. et al. ABySS: A parallel assembler for short read sequence data. *Genome Res.* **19**, 1117–1123 (2009).
60. Li, H. & Durbin, R. Fast and accurate short read alignment with Burrows-Wheeler transform. *Bioinformatics.* **25**, 1754–1760 (2009).
61. Robinson, J. T. et al. Integrative genomics viewer. *Nat Biotechnol.* **29**, 24–26 (2011).
62. Wilm, A. et al. LoFreq: A sequence-quality aware, ultra-sensitive variant caller for uncovering cell-population heterogeneity from high-throughput sequencing datasets. *Nucleic Acids Res.* **40**, 11189–11201 (2012).
63. R Core Team. R: A language and environment for statistical computing. R Foundation for Statistical Computing, Vienna, Austria. https://www.R-project.org/ (2020).

Acknowledgements

The authors wish to thank the UTMB Animal Resource Center for husbandry support of laboratory animals and Drs. Steve Widen and Haiping Hao from the UTMB sequencing core for assistance with sequencing efforts. The authors thank Gilead Sciences for providing remdesivir, Mapp Biopharmaceutical for providing mAb114 and ZMapp, and Regeneron for providing REGN-EB3. This study was supported by the Department of Health and Human Services, National Institutes of Health grant number U19AI109711 and U19AI142785 to T.W.G. and UC7AI094660 for BSL-4 operations support of the Galveston National Laboratory. Opinions, interpretations, conclusions, and recommendations are those of the authors and are not necessarily endorsed by the University of Texas Medical Branch.

Author contributions

T.W.G. conceived and designed the animal challenge experiments. D.J.D. and J.B.G. performed the animal challenges and treatments. A.N.P., C.W., M.B.H., D.J.D., J.B.G., M.B.H., R.W.C., and T.W.G. performed procedures and conducted clinical observations. K.N.A. and V.B. performed the clinical pathology assays. K.N.A. performed the PCR assays. V.B. and J.B.G. performed the EBOV plaque assays. C.W. and R.W.C. performed the sequence analysis. N.S.D. performed the IHC assays. K.A.F. performed gross pathologic, histologic, and immunohistochemical analysis of the data. All authors analyzed the data. A.N.P. and T.W.G. wrote the paper with additions from C.W. and K.A.F. A.N.P., C.W., and K.A.F. prepared the Figures. A.N.P. prepared the Tables. R.W.C. edited the manuscript. All authors had access to the data and approved the final version of the manuscript.

Competing interests

The authors declare no competing interests.

Additional information

Supplementary information The online version contains supplementary material available at https://doi.org/10.1038/s41467-025-59168-5.

Correspondence and requests for materials should be addressed to Thomas W. Geisbert.

Peer review information *Nature Communications* thanks the anonymous reviewers for their contribution to the peer review of this work. A peer review file is available.